Length Scale of Dynamic Heterogeneity in Supercooled D-Sorbitol: Comparison to Model Predictions

XiaoHua Qiu and M. D. Ediger

Department of Chemistry, 1101 University Avenue, University of Wisconsin—Madison, Madison, Wisconsin 53706

Received: August 15, 2002; In Final Form: October 29, 2002

A direct measurement of the length scale of dynamic heterogeneity in supercooled D-sorbitol has been performed using a multidimensional ^{13}C solid-state NMR experiment. Several models predict that the growth of this length scale is linked to the slowing of dynamics as the glass transition is approached from above. At 275 K (T_g + 7 K), 2.5 ± 1.2 nm heterogeneities are detected in sorbitol. This result and recent results of similar measurements on glycerol, *o*-terphenyl, and poly(vinyl acetate) are compared to various models. The only model in quantitative agreement with these experimental data is based upon local fluctuations in the configurational entropy.

I. Introduction

If a liquid does not crystallize as it is cooled, it eventually forms a glassy solid. The transition from liquid to glass, as observed in the laboratory, is a kinetic phenomenon caused by the slowing of molecular motions as the temperature is lowered. Dynamics in some glass formers slow by more than 8 orders of magnitude over a 50 K range above the glass transition temperature T_g. The origin of this dramatic slowing of dynamics is both a long standing question and a matter of considerable current interest.[1] In contrast to first-order phase transitions, there is no significant *structural* change associated with slowing dynamics above T_g. Investigators have looked, without success, for indications of a growing structural length scale that might be expected in analogy with critical phenomena.[2]

Given the failure to identify a structural basis for slowing dynamics as T_g is approached, there has naturally been interest in trying to find a growing dynamic length scale. The apparent activation energy for molecular motion rises rapidly as a liquid is cooled; near T_g, it can be considerably greater than the strength of the covalent bonds that define the individual molecules. The fact that molecules move without breaking covalent bonds argues that, as the temperature is lowered, larger and larger groups of molecules are moving in a cooperative manner. The size of these groups is one candidate for a growing dynamic length scale. This argument is consistent with the Adam-Gibbs model[3] of the glass transition. Unfortunately, no experiment has yet been devised that directly measures the size of these cooperatively rearranging regions.

In the past decade, a number of experiments have demonstrated that dynamics in deeply supercooled liquids are spatially heterogeneous.[4] The length scale of the heterogeneity ξ_{het} can be directly measured with solid-state NMR using the 4D3CP experiment developed by Tracht et al.[5] ξ_{het} is measured in the bulk liquid and does not require the presence of small pores or other types of confinement that have been used to indirectly infer a length scale. There is evidence that ξ_{het} grows with decreasing temperature, from experiments at low temperature[6] and from computer simulations at higher temperatures.[7,8] One can argue that ξ_{het} represents an upper bound for any cooperativity length[5] and it is reasonable to think that these two length scales might be identical.

Given the large number of models of the glass transition that are based on a growing dynamic length scale, an ideal experiment would be to measure ξ_{het} in one material over a wide range of temperature. This has been attempted,[6] but the temperature range that can be covered is too small to allow a definitive test of models. On the other hand, it is possible to study a range of materials and to see which models can successfully predict the observed differences. This is the approach taken in this paper. We note that ξ_{het} is an interesting length scale even if it turns out not to diverge with decreasing temperature. Spatially heterogeneous dynamics have a major influence on the properties of supercooled liquids, being responsible for stretched exponential relaxation,[9] enhanced translational motion,[10] and possibly a new time scale at low temperature.[11] Measurements of ξ_{het} will help us to understand why some liquids exhibit more heterogeneous dynamics than others.

Here we present measurements that allow the determination of ξ_{het} for D-sorbitol at 275 K (T_g + 7 K). Sorbitol is an interesting choice as it is quite fragile (i.e., the relaxation time exhibits a super-Arrhenius temperature dependence) and yet is chemically very similar to glycerol, which is among the strongest of the molecular liquids (i.e., exhibits a more nearly Arrhenius temperature dependence). The sorbitol data are combined with other solid-state NMR results to test various models of dynamic length scales near T_g. Most models do not make quantitatively accurate predictions at this stage of development. One model based on fluctuations in the local configurational entropy is quantitatively consistent with all the experimental data.

II. Experimental Section

D-Sorbitol, ^{13}C labeled at the second carbon, was purchased from Isotope, Inc. The molecular structure of D-sorbitol is $CH_2OH-(CHOH)_4-CH_2OH$. A spin relaxation agent $Cu(NO_3)_2$ was used at a concentration of less than 0.1%. Previous experiments have shown that at such a low concentration the spin relaxation agent does not perturb the dynamics of interest.[6,12] An aqueous solution of D-sorbitol and the relaxation agent

10.1021/jp021888b CCC: $25.00
Published on Web 12/18/2002

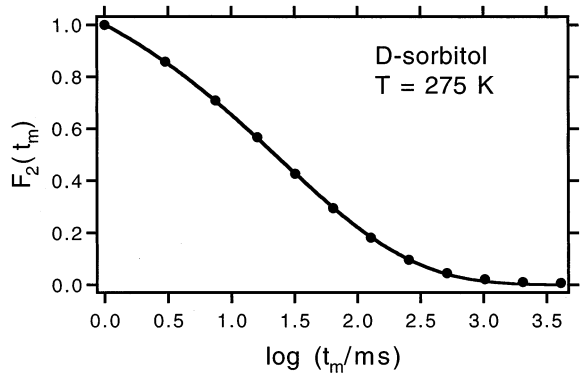

Figure 1. Two-time correlation function describing molecular reorientation for D-sorbitol at 275 K. The fit is a KWW function. The fit parameters are consistent with dielectric relaxation experiments.

was freeze-dried and loaded into a 7.5 mm glass NMR tube. The sample was heated under vacuum to the melting point and held for 1 day. The sample was then quenched to 260 K and sealed under vacuum. The sample was stored at 260 K until beginning the experiment.

The 4D3CP NMR experiment and the 2D echo experiment were performed as previously described.[5,6] All NMR measurements were performed on a Bruker DMX-300 spectrometer with a 7.5 mm double resonance HX probe. The temperature was calibrated by the melting point of water. Temperature stability was monitored by measuring the two-time correlation time at 4 h intervals. The variation in the correlation times indicates that the measurement temperature was constant within 1 K.

III. Results

2D Echo Experiments. Figure 1 shows the two-time correlation function $F_2(t_m)$ for sorbitol at 275 K obtained with an evolution time of 700 μs. The data are well fit to a Kohlrausch−Williams−Watts (KWW) function ($e^{-(t/\tau)^\beta}$) with $\tau = 24$ ms and $\beta = 0.40$. Qualitatively, the F_2 function measures the fraction of ^{13}C−O vectors whose orientation has not changed by at least ~10° at a given time.[13] It is thus similar to other orientation correlation functions and the fitting parameters can be reasonably compared with the results of dielectric relaxation experiments on sorbitol. Wagner and Richert[14] report $\tau_{max} = 140$ ms for dielectric relaxation at 275 K; using the parameters for the Havriliak−Negami fitting functions reported, the KWW β parameter is calculated to be 0.41 ± 0.03.[15] The β parameters from the two techniques are in good agreement. The somewhat smaller correlation time obtained from the NMR experiment is reasonable given that the NMR experiment is sensitive to considerably smaller angular displacements than is dielectric relaxation.

4D3CP Experiments. The 4D3CP experiment, introduced by Tracht et al.,[5] has as an integral part a selection of a slow subensemble, i.e., an ensemble in which molecules have reoriented an unusually small amount in a given time period. The magnetization of this subensemble is then allowed to diffuse into surrounding areas. After various times, ^{13}C spins are interrogated to determine if they are still associated with slow units; at sufficiently long times, the ^{13}C spins are found on sites whose dynamics are characteristic of the entire ensemble. From the time required to leave the slow subensemble, the heterogeneity length scale ξ_{het} can be calculated using an independent measurement of the spin diffusion coefficient.[5] The longer the time required to leave the slow subensemble, the larger is ξ_{het}.[16]

Figure 2 shows the results of the 4D3CP experiment on D-sorbitol at 275 K. Two types of experiments were performed

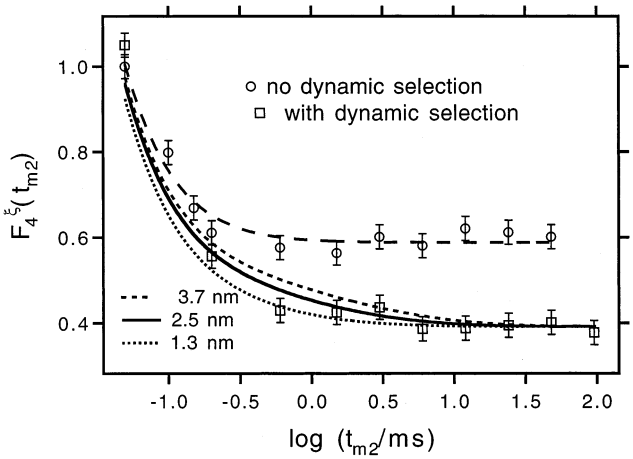

Figure 2. Echo intensities for the 4D3CP experiments as a function of the mixing time t_{m2} for experiments with and without dynamic selection. Fits to the data with dynamic selection are shown for different values of ξ_{het}. At 275 K, ξ_{het} for sorbitol is 2.5 ± 1.2 nm. A fit to the data without dynamic selection is also shown.

(with and without dynamic selection) as discussed below. F_4^ξ as a function of the delay time t_{m2} depends on five variables: the average spacing between ^{13}C atoms (ξ_0), the fraction of reorienting molecules designated as slow (p), the spin diffusion coefficient (D), the characteristic length scale for cross-polarization (a), and the length scale of dynamic heterogeneity (ξ_{het}). In principle, F_4^ξ is also a function of the decay rate of $F_4(t_{m2})$, the 4D echo experiment without cross-polarization. For our experiments, this decay is so slow as to be negligible.

The five parameters in F_4^ξ were determined as follows. ξ_0 is known from the labeling density of the sample to be 0.59 nm. p is equal to the long time limit of the F_4 experiment and is calculated as $F_2(t_{m0})^2/F_2(2t_{m0})$. Using the measured parameters for F_2 (Figure 1) and $t_{m0} = 7$ ms, p is calculated to be 0.66. Two of the remaining parameters, D and a, are determined by fits to the F_4^ξ experiment without dynamic selection. The final parameter, ξ_{het}, is then the sole parameter determined from the F_4^ξ experiment with dynamic selection. Fitting of the results of the 4D3CP experiments was based on eq 8 from the work of Tracht et al.[5] (this equation is reproduced as eq A1 in the Appendix).

The values of D (0.57 nm^2/ms) and a (0.077 nm) obtained from fitting the F_4^ξ curve without dynamic selection (upper curve in Figure 2) are physically reasonable and comparable to other values reported from the 4D3CP experiment. From fitting the F_4^ξ curve with dynamic selection, a value of $\xi_{het} = 2.5 \pm 1.2$ nm is obtained. The solid line in Figure 2 shows the best fit value of ξ_{het}; curves for the bounds on this value, given the error bars on the individual data points, are also shown. Many different attempts were made to fit the data with dynamic selection while allowing for reasonable experimental error in all of the relevant parameters. The range for ξ_{het} cited above also encompasses these fitting attempts.

Because eq A1 must be evaluated numerically, an accurate approximation was developed to facilitate the fitting process. This approximation is described in the Appendix. After the fitting was completed, we verified that any error associated with this approximation was negligible by comparison with the exact solution to eq A1 graciously provided by Stefan Reinsberg. Reinsberg et al. have recently published a more sophisticated method for determining ξ_{het} from F_4^ξ.[12] Their analysis accounts for the correlation hole in the pair distribution function for ^{13}C atoms. On the basis of their comparison of the results of the

TABLE 1: ξ_{het} from 4D3CP NMR for Four Liquids

liquid	ξ_{het} (nm)	T (K)	p	ref
glycerol	1.3 ± 0.5	$T_g + 10$	0.80	6, 12
$T_g = 189$ K	1.1 ± 0.5	$T_g + 14$	0.80	
	1.0 ± 0.5	$T_g + 18$	0.80	
o-terphenyl	2.2 ± 1.0	$T_g + 9$	0.42	12
$T_g = 243$ K	2.3 ± 1.0	$T_g + 9$	0.62	
	2.9 ± 1.0	$T_g + 9$	0.82	
D-sorbitol	2.5 ± 1.2	$T_g + 7$	0.66	this work
$T_g = 268$ K				
poly(vinyl acetate)	3.7 ± 1.0	$T_g + 10$	0.72	5, 12
$T_g = 305$ K				

two fitting methods for the glycerol data, we expect the error associated with the neglect of the correlation hole to be insignificant in comparison to the error bar for ξ_{het} reported here.

IV. Discussion

The measurements of ξ_{het} for sorbitol presented here and the recent publication of measurements for *o*-terphenyl by Reinsberg et al.[12] bring to four the number of liquids for which this quantity has been measured by the 4D3CP NMR technique. In this Discussion, we compare these four measurements with available predictions for ξ_{het}. We choose to use only the 4D3CP measurements for these comparisons for the sake of consistency and also because we believe them to be the most direct measurements available. Other methods of obtaining a dynamic length associated with the glass transition require critical assumptions to be made about the nature of dynamics near T_g or utilize interfaces (e.g., pores[17] or thin films[18]). Although the latter work is very interesting, and important for understanding the properties of nanoscale devices, the presence of an interface is always a significant perturbation and length scales extracted by this approach do not necessarily represent any length scale of the bulk liquid far from an interface.

Although the 4D3CP measurements are the most direct measurements of ξ_{het} available, it is important to note that the characterized regions are assumed in the data analysis to be spherically symmetric. If regions of slow dynamics have shapes that are nonspherical, then the ξ_{het} values reported will be an accurate measurement of the shortest dimension (e.g., diameter for cylinder, thickness for a sheet).[12] This may be a source of ambiguity in some of the comparisons discussed below.

Comparison of ξ_{het} for Four Liquids. Table 1 summarizes the 4D3CP measurements of ξ_{het} reported thus far. In these experiments, the size of regions of unusually slow molecules is determined. "Unusually slow" is defined by the dynamic filter used in the experiment and typically constitutes the slowest 40−80% of the molecules, as indicated by the p values shown in the table. Only for *o*-terphenyl has this variable been systematically explored.[12] Fortunately, the results indicate a relatively weak dependence on p. For comparisons among the four liquids, we use the $p = 0.82$ data for *o*-terphenyl, and we do not consider the slightly different values of p used for the other three liquids to produce any significant ambiguity, given the reported error bars.

We first note that there is no obvious correlation between ξ_{het} and molecular size. Glycerol and the repeat unit of poly(vinyl acetate) are nearly the same size and have a similar degree of internal flexibility, yet the ξ_{het} values differ by a factor of 3. It might be supposed that rather than molecular size, the size of a "bead" representing the smallest rearrangeable unit might be the important parameter. *o*-Terphenyl would certainly have the largest bead size among these molecules, but it does not have the largest ξ_{het}.

TABLE 2: Dynamic Properties of Four Liquids

liquid	fragility (m)	KWW β	T_c(Colby) (K)
glycerol	52[a]	0.68[a,f]	170[d]
o-terphenyl	86[b]	0.52[a]	226[d]
sorbitol	122[a]	0.41[c]	261[e]
poly(vinyl acetate)	73[a]	0.43[a]	282[d]

[a] Fragility/KWW β from dielectric relaxation data in refs 14, 20−22, and 32. [b] Fragility calculated from viscosity data in ref 37 as fit in ref 36. [c] Reference 15. [d] Reference 44. [e] Reference 45. [f] Calculated from β_{CD} using ref 54.

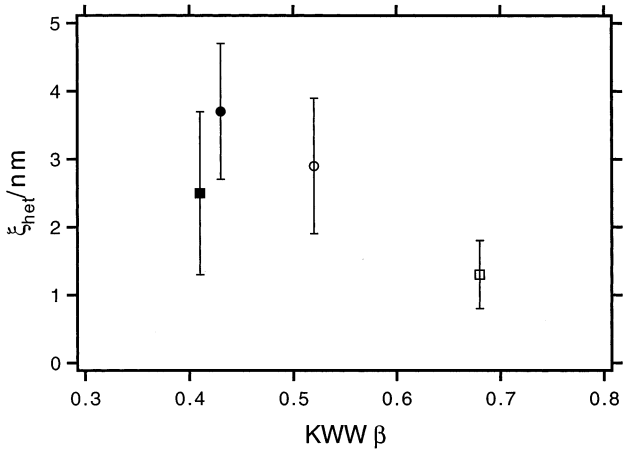

Figure 3. Comparison of measured ξ_{het} values with the KWW β parameter. Broader distributions (i.e., smaller β values) tend to be associated with larger regions of slow molecules. Symbols correspond to sorbitol (■, this work), poly(vinyl acetate) (●, refs 5 and 12), *o*-terphenyl (○, ref 12), and glycerol (□, refs 6 and 12).

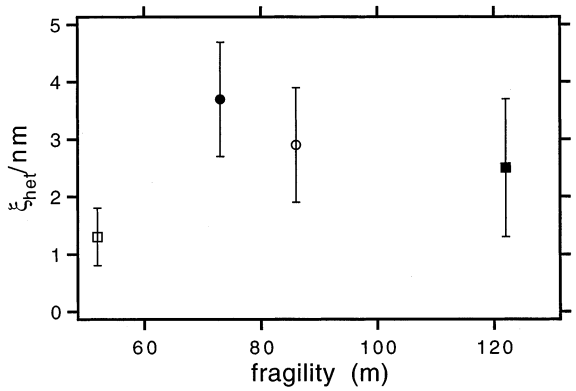

Figure 4. Comparison of measured ξ_{het} values with the fragility parameter m. Symbol codes match Figure 3.

We next compare ξ_{het} values to other parameters that have been associated with spatially heterogeneous dynamics. These parameters are shown in Table 2. Until 1991, it was not clear whether the distribution of α relaxation times characterized by the KWW β parameter should be interpreted as an indication of spatially heterogeneous dynamics.[9] Many experiments are now consistent with the view that nearly the entire width of the observed distribution is due to spatially heterogeneous dynamics.[4,19] One might expect that the size of the regions of heterogeneous dynamics would be correlated with the amplitude of the heterogeneity as represented by β. Figure 3 shows this comparison, indicating some tendency for ξ_{het} to increase as the relaxation time distribution broadens.

Figure 4 shows the correlation between liquid "fragility" and ξ_{het}. We used dielectric relaxation measurements[14,20−22] to define the fragility from the apparent activation energy of the α relaxation at T_g:

$$m = \left.\frac{\mathrm{d}(\log \tau)}{\mathrm{d}(T_g/T)}\right|_{T_g} \quad (1)$$

Because fragile liquids generally exhibit smaller KWW β parameters[23] and hence greater spatial heterogeneity than strong liquids, one might have anticipated that ξ_{het} would be positively correlated with fragility. Clearly the data do not exhibit any simple pattern.

Finally, we consider ξ_{het} in terms of chemical functionality. Sorbitol was chosen for these studies partly because it is essentially a dimer of glycerol, one of the other molecules studied with the 4D3CP method. Despite their similar chemical functionality, these two molecules have very different fragilities and ξ_{het} values.

Macroscopic Fluctuation Models. From one viewpoint, spatially heterogeneous dynamics are simply the consequence of fluctuations that occur in equilibrium liquids. If we knew what the relevant fluctuating quantity was (e.g., density or configurational entropy), and how those fluctuations produced variations in the dynamics, then we could calculate the characteristics of the dynamic domains. The simplest approach along these lines, described by Moynihan and Schroeder,[24] is to assume that ξ_{het} is large enough that a continuum description of the liquid is adequate. In this approximation, the amplitude of density fluctuations associated with the glass transition depends on only the average density, the temperature, the change in compressibility at the glass transition, and the size of the volume considered. The local relaxation time associated with a density fluctuation of a certain amplitude is calculated by assuming that each small volume of the liquid shifts its dynamics with density in the same way as the bulk liquid. If we assume that this description is correct, we can use the observed distribution of relaxation times (e.g., the KWW β) to calculate ξ_{het}.

We can compare the 4D3CP measurements of ξ_{het} to four different predictions based on the above approach. Moynihan and Schroeder present two approaches; one is based on density fluctuations as described in the previous paragraph (eq 19 in ref 24) and the other assumes that fluctuations in the local specific configurational entropy (rather than the density) are responsible for the observed variations in dynamics (eq 11 in ref 24).[25] Later, Ediger[26] modified these two approaches by calculating $\mathrm{d}(\log \tau)/\mathrm{d}\rho$ and $\mathrm{d}(\log \tau)/\mathrm{d}s$ directly from experimental data without making any assumptions about the validity of the free volume or Adam−Gibbs models. Ediger's predictions of ξ_{het} based upon density and configurational entropy fluctuations are calculated from eqs 4 and 6 in ref 26, respectively.[25] The material parameters needed as input for these four predictions were found in the following references and are provided in the Supporting Information: glycerol,[20,24,27−30] poly(vinyl acetate),[24,31−33] *o*-terphenyl,[21,34−37] sorbitol.[14,35,38−40]

Figure 5 shows the comparison of the four calculations of ξ_{het} based on density and configurational entropy fluctuations to the values measured with the 4D3CP method. The ordinate shows the experimental measurements, with error bars, along with the predictions of these four approaches. A prediction that lies within the experimental error bars is taken as quantitatively consistent. Clearly, the two equations based on density fluctuations deviate significantly from the measured values and have no predictive power. In contrast, values predicted on the basis of configurational entropy fluctuations are close to the measured values. It should be noted that due to uncertainty in the input parameters, there is some uncertainty in the predicted values as well as the experimental results. The Moynihan/Schroeder prediction based on entropy fluctuations is uncertain to within about 15%, whereas the Ediger prediction based on entropy fluctuations is uncertain to within 20%. Given these uncertainties in the calculated quantities, the Moynihan/Schroeder entropy prediction is consistent with all the 4D3CP data except glycerol whereas the Ediger entropy prediction is (just barely) consistent with all the 4D3CP data. According to this model, ξ_{het} is given by

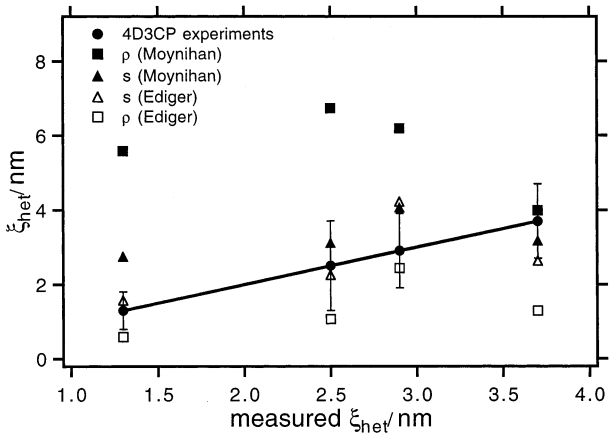

Figure 5. Comparison of measured ξ_{het} values with values predicted by models based on flucuations in the density or the specific configurational entropy. The models based on fluctuations in the specific configurational entropy best reproduce the data. Predictions lying within the experimental error bars are consistent with the experiments. Results for the different liquids are plotted according to their measured ξ_{het} values: from left, glycerol, sorbitol, *o*-terphenyl, and poly(vinyl acetate).

$$(\xi_{het})^3 = \frac{k\Delta c_p}{\alpha^2 \nu \langle(\delta \log \tau)^2\rangle}\left[\frac{\mathrm{d}\langle \log \tau\rangle}{\mathrm{d}p}\right]_T^2 \quad (2)$$

where α, ν, and $\langle(\delta \log \tau)^2\rangle$ are the thermal expansivity, the specific volume, and the variance of the relaxation time distribution, respectively.

Donth and co-workers have presented a related approach based on temperature fluctuations,[35] sometimes interpreted as fictive temperature fluctuations.[41] On the basis of results reported in the literature, we can make comparisons between Donth's predictions and some of the 4D3CP values for ξ_{het}. From data and procedures in ref 42, we calculate ξ_{Donth} for glycerol as 2.4 nm (T_g + 10 K) and 2.1 nm (T_g + 18 K). These values are about 2 times larger than the 4D3CP measurements at 1.3 and 1.0 nm, respectively. For poly(vinyl acetate), we interpolate between ξ_{Donth} values at two temperatures[35] to obtain 2.9 nm at T_g + 10 K, which agrees with the experimental value given the error bar. ξ_{Donth} for OTP at T_g + 6 K (3.0 nm)[35] is similar to the 4D3CP measurement at a temperature 3 K higher.

Dynamic Scaling Model. Colby recently presented a dynamic scaling model of the glass transition, which accounts for the non-Arrhenius temperature dependence of fragile glass formers through a growing cooperativity length ξ.[43] The model predicts[44] that

$$\xi/r_0 = \left[\frac{T - T_c}{T_c}\right]^{-3/2} \quad (3)$$

Here T_c is obtained independently from a power law fit to the experimental relaxation times as a function of temperature. T_c values[44,45] are given in Table 2. Erwin and Colby[44] have compared this prediction with 4D3CP measurements of ξ_{het} for glycerol, *o*-terphenyl, and poly(vinyl acetate), choosing r_0 =

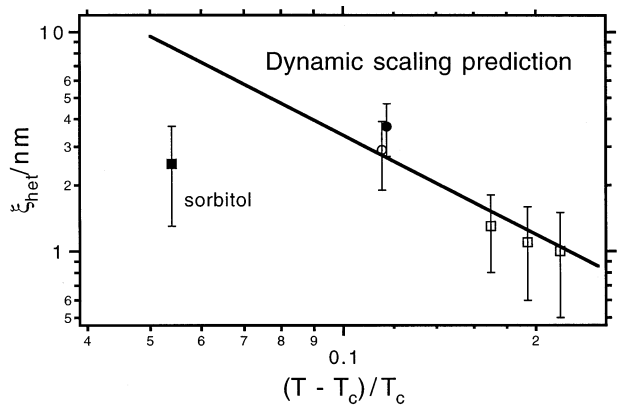

Figure 6. Comparison of measured ξ_{het} values with the dynamic scaling prediction of Colby. Symbol codes match Figure 3; glycerol data (□) are shown for three temperatures.

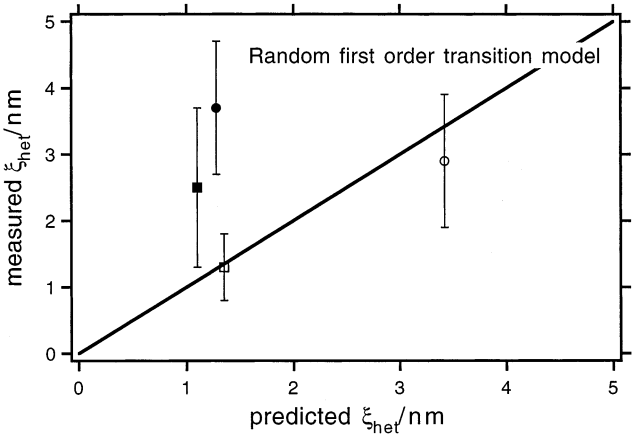

Figure 7. Comparison of measured ξ_{het} values with predictions based on the random first-order transition theory of Wolynes and co-workers. A successful prediction requires the experimental error bar to intersect the line of slope 1. Symbol codes match those in Figure 3.

0.11 nm. In Figure 6, we extend this comparison to include sorbitol. As noted in ref 44, the data for glycerol, *o*-terphenyl, and poly(vinyl acetate) are in quite good agreement with the model. We offer no explanation for why the sorbitol value does not agree with the model but do note that it is the small value of $(T - T_c)/T_c$ that sets it apart from the other fragile glass formers (*o*-terphenyl and poly(vinyl acetate)). In constructing Figure 6, we followed ref 44 in choosing a single value of r_0 for all liquids; clearly, this constraint could be relaxed.

Microscopic/Mesoscopic Theories. About 15 years ago, Wolynes, Kirkpatrick, and Thirumalai developed a random first-order transition theory to explain the glass transition.[46] Recently, Xia and Wolynes[47] have constructed a microscopically motivated model of dynamics that makes specific predictions about the size of rearranging regions; in ref 47 they compare this prediction to ξ_{het} for poly(vinyl acetate). Their expression, as modified by more recent work,[48] can be written as

$$\xi/r_0 = 0.51(\ln \tau/\tau_0)^{2/3} \quad (4)$$

Here r_0 represents the lattice spacing for "beads" or mobile units and τ_0 is the prefactor from the Vogel−Tamman−Fulcher (VTF) equation; VTF parameters for these liquids are given in the Supporting Information. We have compared this prediction to the ξ_{het} values for four liquids in Figure 7. In making this comparison, we represent *o*-terphenyl and glycerol with 3 and 6 beads, respectively; the same choices were made in ref 47. We represent sorbitol and a poly(vinyl acetate) monomer by 12 and 5 beads, respectively, following Wunderlich's criteria.[49] Although the predictions for glycerol and *o*-terphenyl are in excellent agreement with the experimental data, deviations are observed for sorbitol and poly(vinyl acetate). Other definitions of a bead would yield different results. For example, defining a bead to ensure that the predicted relationship between Δc_p and fragility from reference 47 is obeyed increases the predicted values of ξ_{het} for sorbitol and poly(vinyl acetate) by about 0.9 nm while not changing the predictions for glycerol and *o*-terphenyl. This definition of a bead produces predictions for three of the four liquids that agree with experiment given the error bars; the predicted value for poly(vinyl acetate) remains too small (2.1 nm). Clearly the definition of a bead is critical for this comparison.

Kivelson, Tarjus, and co-workers[50] have developed a theory of the glass transition based on the growth of frustration-limited domains. They predict[51] a characteristic domain size L^* as

$$\frac{L^*}{a_0} \approx B^{1/2}\left[1 - \frac{T}{T^*}\right]^{2/3} \quad (5)$$

Here B and T^* are parameters obtained by fitting the temperature dependence of relaxation times. According to ref 51, the "≈" sign indicates that constants of order 1 were set equal to 1 to obtain this equation. To compare eq 5 with our measurements, we obtained B and T^* values for glycerol, *o*-terphenyl, and poly(vinyl acetate) from ref 52. The molecular diameter, a_0, was calculated from the density. Using these parameters, we calculated L^* for these three liquids from eq 5. The results are 2.4 nm for glycerol, 6.1 nm for *o*-terphenyl, and 3.7 nm for poly(vinyl acetate). Although the value for poly(vinyl acetate) is in excellent agreement with 4D3CP measurements of ξ_{het}, the other two predicted values are a factor of 2 too large. This disagreement may be related to the approximation in developing eq 5, but in this case those prefactors must be material specific.

V. Concluding Remarks

We have used the 4D3CP solid-state NMR experiment to measure the length scale of spatially heterogeneous dynamics in supercooled D-sorbitol near T_g. The ξ_{het} value of sorbitol, when combined with values from similar measurements for three other liquids, allows tests of a number of predictions of this quantity. The only prediction that is quantitatively consistent with all the 4D3CP data is based upon local fluctuations in the configurational entropy.

Although the above comparison is a useful way to discriminate among various approaches, many of the predictions for ξ_{het} contain material specific prefactors that are not necessarily known well. If the temperature dependence of ξ_{het} could be compared against these predictions, this source of ambiguity would be eliminated and a further significant test would be possible. At this stage of development, the 4D3CP NMR measurement cannot be performed over a wide temperature range. An alternate approach to obtaining the temperature dependence of ξ_{het} would be to combine the existing 4D3CP measurements near T_g with atomistic molecular dynamics simulations at high temperatures; these together would span a 80−100 K range. MD simulations on model systems have been useful for characterizing the length scale of dynamic heterogeneity,[7,8] and recent atomistic simulations with carefully tested force fields have been found to produce dynamics in excellent agreement with experimental measurements.[53] A comprehensive test of predictions for the temperature dependence of ξ_{het} seems accessible through this route.

Acknowledgment. We thank Stefan Reinsburg for detailed, helpful conversations about the 4D3CP experiment and for his help with the fitting of experimental results. We thank George Zografi, Marv Kontney, and Tom Farrar for their assistance with these experiments and Ranko Richert, John Fourkas, Ernst Donth, and Peter Wolynes for helpful conversations. This work was supported by the National Science Foundation (NSF-CHE 9988629).

Supporting Information Available: A table with properties of glycerol, *o*-terphenyl, poly(vinyl acetate), and D-sorbitol used to evaluate the models. This material is available free of charge via the Internet at http://pubs.acs.org.

Appendix

Tracht et al. have shown that F_4^{ξ} can be expressed as follows:

$$F_4^{\xi}(t_{m2}) = \frac{1}{(4\pi D t_{eff})^{3/2}} \int \exp(-\mathbf{r}^2/4Dt_{eff}) \times \left[\exp(-\mathbf{r}^2/2a^2) F_4(t_{m2}) + \frac{1}{\xi_0^{\,3}} \int \exp(-(\mathbf{r}-\mathbf{r}_c)^2/2a^2)(p + (1-p)\exp(-2|\mathbf{r}_c|/\xi_{het}) y(t_{m2}))\, d\mathbf{r}_c \right] d\mathbf{r} \quad \text{(A1)}$$

Here $t_{eff} = t_{m2} + a^2/2D$ and $y(t_{m2}) = [F_4(t_{m2}) - F_4(\infty)]/[1 - F_4(\infty)]$. Other variables are described in the text. Parameter a is expected to be on the order of 0.1 nm. When ξ_{het} greatly exceeds this value, as is generally expected to be the case, the integrand $\exp(-(\mathbf{r} - \mathbf{r}_c)^2/2a^2)$ can be replaced by a delta function $\delta(\mathbf{r} - \mathbf{r}_c)$. With this substitution, the following expression is obtained without further approximation:

$$F_4^{\xi}(t_{m2}) = \frac{F_4(t_{m2})}{(1 + 2Dt_{eff}/a^2)^{3/2}} + (2\pi)^{3/2}(a/\xi_0)^3 \times \{p + (1-p)y(t_{m2})[\exp(z^2)[(2z^2+1)\,\mathrm{erfc}(z) - 2z/\sqrt{\pi}]\} \quad \text{(A2)}$$

Here $z = (4Dt_{eff})^{1/2}/\xi_{het}$. For the case of no dynamic selection ($p = 1$), this equation exactly reproduces eq A1 above. In our tests of eq A2, as long as a was 0.1 nm or less, the calculated values of F_4^{ξ} matched the predictions of eq A1 within 0.01, when F_4^{ξ} was normalized to 1 and ξ_{het} was in the range of 1−3 nm.

References and Notes

(1) See recent reviews: Ediger, M. D.; Angell, C. A.; Nagel, S. R. *J. Phys. Chem.* **1996**, *100*, 13200. Debenedetti, P. G.; Stillinger, F. H. *Nature* **2001**, *401*, 259. Angell, C. A.; Ngai, K. L.; McKenna, G. B.; McMillan, P. F.; Martin, S. W. *J. Appl. Phys.* **2000**, *88*, 3113.

(2) Leheny, R. L.; Menon, N.; Nagel, S. R.; Price, D. L.; Suzaya, K.; Thiyagarajan, R. *J. Chem. Phys.* **1996**, *105*, 7783.

(3) Adam, G.; Gibbs, J. H. *J. Chem. Phys.* **1965**, *43*, 139.

(4) Ediger, M. D. *Annu. Rev. Phys. Chem.* **2000**, *51*, 99. Sillescu, H. *J. Non-Cryst. Solids* **1999**, *243*, 81. Richert, R. *J. Phys.: Condens. Matter* **2002**, *14*, R703.

(5) Tracht, U.; Wilhelm, M.; Heuer, A.; Feng. H.; Schmidt-Rohr, K.; Spiess, H. W. *Phys. Rev. Lett.* **1998**, *81*, 2727. Tracht, U.; Wilhelm, M.; Heuer, A.; Spiess, H. W. *J. Magn. Reson.* **1999**, *140*, 460.

(6) Reinsberg, S. A.; Qiu, XH.; Wilhelm, M.; Spiess, H. W.; Ediger, M. D. *J. Chem. Phys.* **2001**, *114*, 7299.

(7) Scheidler, P.; Kob, W.; Binder, K.; Parisi, G. *Philos. Mag. B* **2002**, *82*, 283.

(8) Lacevic, N.; Starr, F. W.; Schroder, T. B.; Novikov, V. N.; Glotzer, S. C. *Phys. Rev. E* **2002**, *66*, 030101.

(9) Schmidt-Rohr, K.; Spiess, H. W. *Phys. Rev. Lett.* **1991**, *66*, 3020.

(10) Cicerone, M. T.; Wagner, P. A.; Ediger, M. D. *J. Phys. Chem. B* **1997**, *101*, 8727.

(11) Wang, C. Y.; Ediger, M. D. *J. Phys. Chem. B* **1999**, *103*, 4177.

(12) Reinsberg, S. A.; Heuer, A.; Doliwa, B.; Zimmermann, H.; Spiess, H. W. *J. Non-Cryst. Solids* **2002**, *307−310*, 208.

(13) More precisely, the correlation function monitors the change in resonance frequency associated with the reorientation of the chemical shift tensor.

(14) Wagner, H.; Richert, R. *J. Phys. Chem. B* **1999**, *103*, 4071.

(15) Richert, R. Private communication, 2002.

(16) The time required to diffuse away from the slow subensemble is considerably shorter than τ_{ex}, the characteristic lifetime of the slow subensemble. Thus slow molecules do not become fast molecules on the time scale of the diffusion experiment.

(17) Arndt, M.; Stannarius, R.; Gorbatschow, W.; Kremer, F. *Phys. Rev. E* **1996**, *54*, 5377.

(18) Forrest, J. A.; Dalnoki-Veress, K. *Adv. Colloid Interface Sci.* **2001**, *94*, 167.

(19) Bohmer, R.; Chamberlin, R. V.; Diezemann, G.; Geil, B.; Heuer, A.; Hinze, G.; Kuebler, S. C.; Richert, R.; Schiner, B.; Sillescu, H.; Spiess, H. W.; Tracht, U.; Wilhelm, M. *J. Non-Cryst. Solids* **1998**, *235−237*, 1.

(20) Schneider, U.; Lunkenheimer, P.; Brand, R.; Loidl, A. *J. Non-Cryst. Solids* **1998**, *235−237*, 173.

(21) Naoki, M.; Endou, H.; Matsumoto, K. *J. Phys. Chem.* **1987**, *91*, 4169.

(22) Wagner, H.; Richert, R. *Polymer* **1997**, *38*, 255.

(23) Bohmer, R.; Ngai, K. L.; Angell, C. A.; Plazek, D. J. *J. Chem. Phys.* **1993**, *99*, 4201.

(24) Moynihan, C. T.; Schroeder, J. *J. Non-Cryst. Solids* **1993**, *160*, 52.

(25) To calculate ξ_{het} from these equations, set $V = (\xi_{het})^3$ and solve for ξ_{het}.

(26) Ediger, M. D. *J. Non-Cryst. Solids* **1998**, *235−237*, 10.

(27) Schulz, A. *J. Chim. Phys.* **1954**, *51*, 324.

(28) Gilchrist, A.; Earley, J. E.; Cole, R. H. *J. Chem. Phys.* **1957**, *26*, 196.

(29) Johari, G. P.; Whalley, E. *Faraday Symp. Chem. Soc.* **1972**, *3*, 23.

(30) Moynihan, C. T.: Boesch, L. P.; Laberge, N. L. *Phys. Chem. Glasses* **1973**, *14*, 122.

(31) McKenna, G. In *Comprehensive Polymer Science*; Booth, C., Price, C., Eds.; Pergamon: Oxford, U.K., 1990; Vol. 2, p 311.

(32) Richert, R. *Physica A* **2000**, *287*, 26.

(33) O'Reilly, J. M. *J. Polym. Sci.* **1962**, *57*, 429.

(34) Naoki, M.; Koeda, S. *J. Phys. Chem.* **1989**, *93*, 948.

(35) Hempel, E.; Hempel, G.; Hensel, A.; Schick, C.; Donth, E. *J. Phys. Chem. B* **2000**, *104*, 2460.

(36) Cicerone, M. T.; Ediger, M. D. *J. Phys. Chem.* **1993**, *97*, 10489.

(37) Plazek, D. J.; Bero, C. A.; Chay, I. C. *J. Non-Cryst. Solids* **1994**, *172−174*, 181.

(38) Naoki, M.; Katahira, S. *J. Phys. Chem.* **1991**, *95*, 431.

(39) Naoki, M.; Ujita, K.; Kashima, S. *J. Phys. Chem.* **1993**, *97*, 12356.

(40) Olsen, N. B. *J. Non-Cryst. Solids* **1998**, *235*, 399.

(41) Sillescu, H. *Acta Polym.* **1994**, *45*, 1.

(42) Korus, J.; Hempel, E.; Beiner, M.; Kahle, S.; Donth, E. *Acta Polym.* **1997**, *48*, 369.

(43) Colby, R. H. *Phys. Rev. E* **2000**, *61*, 1783.

(44) Erwin, B. M.; Colby, R. H. *J. Non-Cryst. Solids* **2002**, *307−310*, 225.

(45) Colby, R. Private communcation, 2002.T_c value for sorbitol.

(46) Kirkpatrick, T. R.; Wolynes, P. G. *Phys. Rev. A* **1987**, *35*, 3072. Kirkpatrick, T. R.; Thirumalai, D. *Phys. Rev. Lett.* **1987**, *58*, 2091.

(47) Xia, X.; Wolynes, P. G. *Proc. Natl. Acad. Sci. U.S.A.* **2000**, *97*, 2990.

(48) Lubchenko, V.; Wolynes, P. G. *Phys. Rev. Lett.* **2001**, *87*, 195901. Equation 4 predicts ξ_{het} values 1.3 times larger than the prediction in ref 47.

(49) Wunderlich, B. *J. Phys. Chem.* **1960**, *64*, 1052.

(50) Kivelson, D.; Kivelson, S. A.; Zhao, X.; Nussinov, Z.; Tarjus, G. *Physica A* **1995**, *219*, 27.

(51) Viot, P.; Tarjus, G.; Kivelson, D. *J. Chem. Phys.* **2000**, *112*, 10368.

(52) Kivelson, D.; Tarjus, G. *J. Non-Cryst. Solids* **1998**, *235−237*, 1998.

(53) Smith, G. D.; Borodin, O.; Bedrov, D.; Paul, W.; Qiu, XH.; Ediger, M. D. *Macromolecules* **2001**, *34*, 5192.

(54) Lindsey, C. P.; Patterson, G. D. *J. Chem. Phys.* **1980**, *73*, 3348.